

# Influence of radiation on Voltage Terminating Structure of silicon relativistic particle detectors

**N Fadeeva<sup>1,2</sup>, V Eremin<sup>1</sup>, E Verbitskaya<sup>1</sup> and E Terukov<sup>1</sup>**

<sup>1</sup>Ioffe Physical-Technical Institute of the Russian Academy of Sciences,  
Polytekhnicheskaya str. 26, 194021 St. Petersburg, Russia

<sup>2</sup>Saint Petersburg Electrotechnical University, Prof. Popov str. 5, 197376 St. Petersburg, Russia

E-mail: fadeevanadezda@gmail.com

**Abstract.** Semiconductor radiation detectors are widely applied in high energy physics experiments. The largest particle colliders use silicon detectors with the total area of hundreds square meters that enhances the requirement to their stable long-term operation. This is provided by incorporating the floating p<sup>+</sup> rings surrounding the sensitive area of the p<sup>+</sup>-n-n<sup>+</sup> detectors (VTS – Voltage Termination Structure), that prevents an electric breakdown. The physical model of VTS operation in high-resistivity p<sup>+</sup>-n-n<sup>+</sup> silicon radiation detectors developed in the study uses an approach of the current injection through the ring spacings of VTS that may occur under a certain electric field distribution. This leads to a strict stabilization of the ring potentials. Investigation of the potential distribution in VTS of silicon detectors irradiated with 1 MeV neutrons up to a fluence of  $5 \times 10^{15}$  n<sub>eq</sub>/cm<sup>2</sup> was carried out. It was shown that the change of the electric field profile in the detector bulk with increasing radiation fluence is a key factor for the potential distribution. At fluences less than  $5 \times 10^{14}$  n<sub>eq</sub>/cm<sup>2</sup> the potential distribution in VTS is governed by the punchthrough mechanism, whereas at higher fluences it is controlled by the bulk generation current and interaction with radiation induced deep levels.

## 1. Introduction

Silicon detectors which are used in high luminosity hadron colliders (such as the Large Hadron Collider (LHC) at CERN (Switzerland), and TEVATRON at the Fermi laboratory (USA)) can require high operational voltages (in excess of 500 V) to maintain full depletion and effective collection of nonequilibrium charge carriers even at irradiation fluences more than 10<sup>14</sup> n<sub>eq</sub>/cm<sup>2</sup>.

Radiation detectors of low-energy photons and short-range particles are based on the structures with shallow junctions (less than 1 μm) processed by ion implantation. Therefore, detector operation at high reverse bias results in significant electric fields at the p-n junction periphery that is accompanied by abrupt increase in the reverse current and subsequent breakdown.

To prevent low voltage breakdown at the junction periphery, i.e. stabilize the detector I-V characteristics, the junction active region is surrounded by potential dividers with isolated ring p-n junctions (VTS – voltage terminating structures) that gradually reduce the potential from the central active region towards the periphery [1]. Operation of VTS was studied earlier for the diodes processed on silicon with a resistivity  $\rho$  of tens and hundreds Ω×cm and p-n junction depths of tens micrometers [2-7]. Existing models for the VTS calculation are based on the electrostatic approach to the problem



Content from this work may be used under the terms of the [Creative Commons Attribution 3.0 licence](#). Any further distribution of this work must maintain attribution to the author(s) and the title of the work, journal citation and DOI.

in which it is postulated that the electric field is transferred from the inner structural element to an adjacent one when the space charge regions (SCRs) of both elements touch each other.

A principal disadvantage of the electrostatic model becomes clear when it is applied to radiation detectors on high resistivity silicon. For example, at the typical distances of 10-30  $\mu\text{m}$  between the structural elements and n-type silicon resistivity in the range of 3-20  $\text{k}\Omega\text{-cm}$ , SCRs of the individual rings touch each other even at a zero bias due to a built-in potential. According to the electrostatic model, all rings in such structures should have close potentials, i.e. the VTS appears to be inconsistent. This contradicts with the practice of VTS operation in radiation detectors.

It is necessary to maintain stable operation in detectors irradiated to the fluences exceeding  $10^{14} \text{n}_{\text{eq}}/\text{cm}^2$ . One of the aspects of solving this problem is related with the influence of the high fluences of relativistic particles on VTS. Irradiation of silicon with high energy particles leads to the formation of the radiation defects, including those that have energy levels in the band gap, and so are electrically active. In turn, this results in the trapping of nonequilibrium charge carriers during their drift to the collection electrodes, which modifies the distribution of the electric field in the sensitive area of the detector and gives rise to a decrease in the amplitude of the detector signal. Generation of the equilibrium charge carriers via midgap energy levels of radiation induced defects brings to an increase in the leakage current of the detector and a decrease in signal-to-noise ratio.

In this paper we consider a physical model of VTS operation of nonirradiated and neutron irradiated detectors which is based on the injection mechanism of current flow through the ring spacings. The measurements were performed for the samples manufactured within the frames of a project for the development of proton detectors for the TOTEM experiment at CERN. The studies are focused on the development of radiation hard detectors for the LHC upgrade and are also important for the development of silicon detectors for the future experiments within the FAIR program at Research Center GSI (Germany).

## 2. Experimental

A photograph of  $\text{p}^+$ -n junction detector (top view) and its fragment with VTS are shown in figure 1. Detectors were processed on n-type FZ Si wafers manufactured by TOPSIL, Denmark. Si resistivity

was  $7 \text{k}\Omega\text{-cm}$ . All structures had the same topology with the central  $\text{p}^+$  area (pad)  $5 \times 5 \text{ mm}^2$ . The VTS consisted of four closed floating  $\text{p}^+$  rings separated by ring spacings. The surface of the ring spacings was passivated with a  $\text{SiO}_2$  layer. The ohmic side was an  $\text{n}^+$  sheet implant. The thickness of the structures was  $300 \mu\text{m}$ . Detectors were irradiated with 1 MeV neutrons up to a fluence of  $5 \times 10^{15} \text{n}_{\text{eq}}/\text{cm}^2$ , which, in fact, covers the expected range of radiation fluences for Si tracking detectors in the principal experiments in the LHC after a planned increase in the beam intensity.

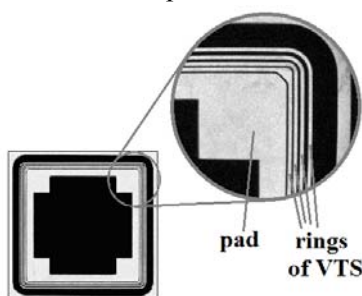


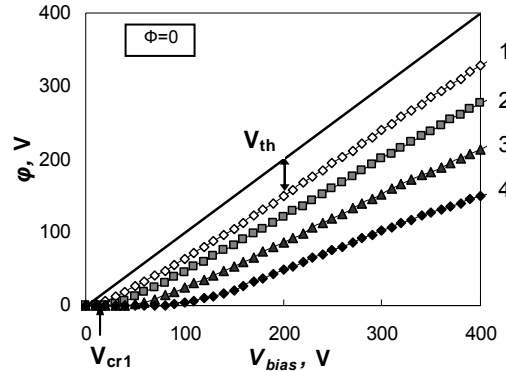
**Figure 1.** A photograph of the detector.

with microprobes and a Keithley 487 Picoammeter/Voltage Source. The probe was sensitive to the potential and had the resistance  $10^{12} \Omega$ , which ensured the conditions of floating potential for a ring; the central  $\text{p}^+$ -n junction was reverse biased with the voltage  $V_{\text{bias}}$  at a grounded  $\text{n}^+$  contact. I-V characteristics of ring spacings were measured at bias voltage  $V_{\text{bias}}$  applied to the pad and the voltage  $\Delta V$  applied to the ring spacing. All measurements were performed at a temperature  $20^\circ\text{C}$ .

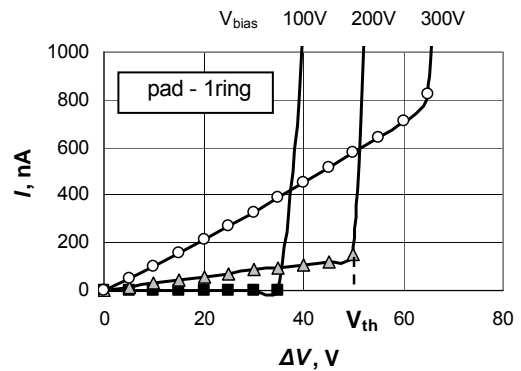
## 3. Experimental results

Figure 2 shows the dependences of the potentials  $\varphi$  in VTS on the reverse bias  $V_{\text{bias}}$  for nonirradiated detectors. The magnitudes of negative voltages and potentials are given in the figures and text. The solid line shows the potential of the pad, the numbers of curves correspond to the numbers of the rings.

It can be seen that for a nonirradiated detector the potentials of all rings monotonically increase with the voltage  $V_{bias}$  applied to the pad. In this case, the potential of an individual ring begins to increase at a certain critical voltage  $V_{cr}$  which significantly exceeds the built-in potential at the  $p^+$ - $n$  junction ( $\sim 0.6$  V), which is sufficient for joining the SCRs of the adjacent  $p^+$ - $n$  junctions in the electrostatic model.



**Figure 2.** Ring potentials of nonirradiated detector. The solid line shows the potential of the pad, the numbers of curves correspond to the numbers of the rings.



**Figure 3.** I-V characteristic of the pad-1 ring spacing at bias  $V_{bias} = 100, 200$  and  $300$  V.

Figure 3 shows the dependences of the pad – 1<sup>st</sup> ring spacing current  $I$  for nonirradiated detector on the voltage  $\Delta V$  applied to the spacing. Measurements were performed at three various bias  $V_{bias}$ , 100, 200 and 300 V, respectively. There are two regions in the characteristics: a region with a weakly increasing low current and a region of a sharp current increase at the threshold voltage  $V_{th}$ . The former one is associated with leakages of ring spacing insulation due to the ohmic surface conductivity and generation-recombination processes at the Si/SiO<sub>2</sub> interface [8]. The sharp current increase at the  $V_{th}$  is not a breakdown due to the fact it can be reproduced many times, so it is a beginning of the injection current. Indeed, the structure with ring spacings is symmetric and the current increase corresponds to forward biasing of one of the  $p^+$ - $n$  junctions (punch-through).

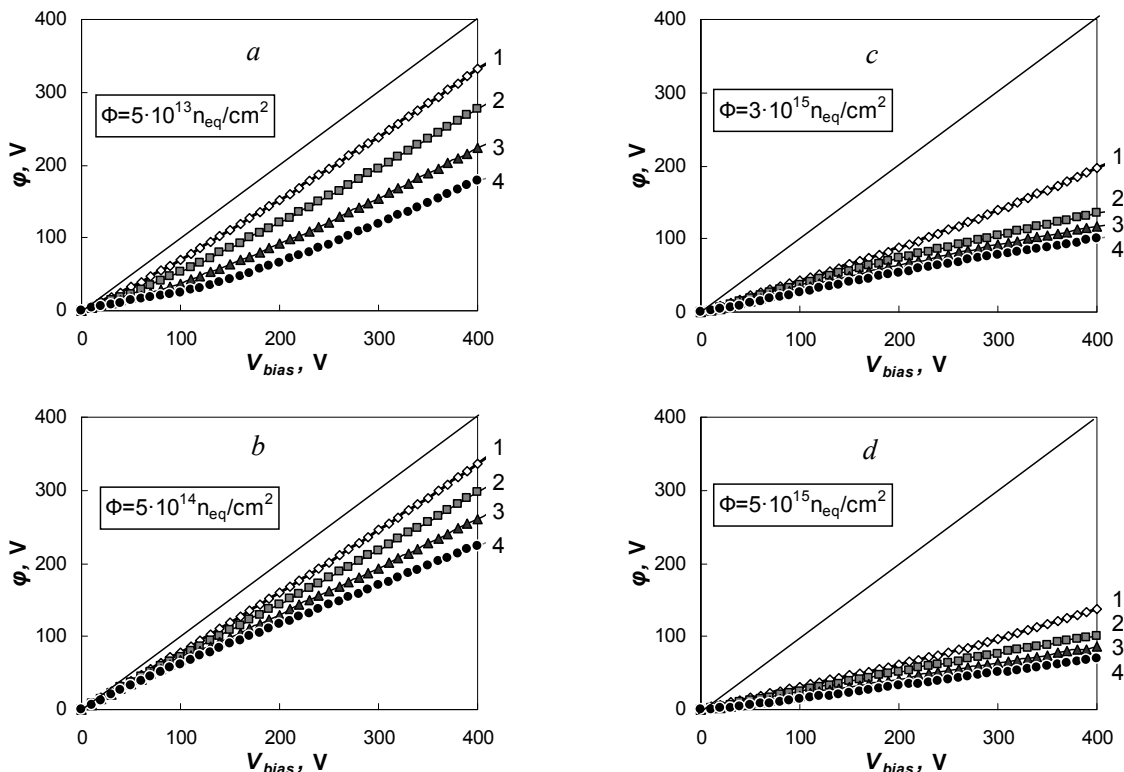
It should be noted that the value of the threshold voltage  $V_{th}$  on I-V characteristic of the pad – 1<sup>st</sup> ring spacing (figure 3) equals to the potential difference between the pad and the 1<sup>st</sup> ring at a certain bias  $V_{bias}$  (figure 2). Therefore, potential distribution in VTS is controlled by the injection current in a ring spacing.

Figure 4 shows the dependences of the potentials  $\varphi$  at VTS rings on the reverse bias  $V_{bias}$  for detectors irradiated by neutrons in the range of fluences from  $5 \times 10^{13}$  to  $5 \times 10^{15}$  n<sub>eq</sub>/cm<sup>2</sup>. As the fluence increases the value of the critical voltage  $V_{cr}$  for all rings decreases and becomes equal to zero at a dose of  $5 \times 10^{13}$  n<sub>eq</sub>/cm<sup>2</sup> (figure 4 (a)). For detectors irradiated to a fluence  $5 \times 10^{14}$  n<sub>eq</sub>/cm<sup>2</sup> (figure 4 (b)) the potentials at all rings increase in the entire range of bias  $V_{bias}$  in comparison with ones for detectors irradiated to lower fluences. At low bias  $V_{bias}$  (0 – 200 V) the ring potentials are close to each other and effective dividing of the potentials is lacking. As the fluence further increases (figures 4 (c), 4 (d)), the potentials of all rings become the same in the entire range of  $V_{bias}$ , while the voltage drop between the pad and the 1<sup>st</sup> ring considerably increases.

#### 4. The model of the potential distribution in VTS of nonirradiated detectors

The potential distribution in VTS of nonirradiated detectors is described in terms of an injection model of current flows through the ring spacings. At a zero bias SCR corresponding to the built-in potential of the pad junction and the 1<sup>st</sup> ring are joined and a potential minimum in the central of spacing is observed. As the bias increases, the SCR of the pad junction extends and the potential minimum shifts to the ring, the potential of which remains zero. The existing potential barrier for the holes prevents

their transport between the  $p^+$  regions and the ring remains insulated from the pad, that corresponds to the region  $\Delta V < V_{cr}$ . This state will retain until the potential barrier will decrease to a value allowing hole injection from the ring to the spacing. The ring spacing resistance will sharply drop. The punch-through of the ring spacing occurs and the ring potential becomes different from zero. A further increase in  $V_{bias}$  brings about an increase in the ring potential. The conditions required for a punch-through of the ring spacing depend on the electric field distribution in the ring spacing and are determined by the competition between the normal and tangential (parallel to the surface of the ring spacing) vectors of the electric field. Injection is stimulated by the tangential component of the electric field, whereas the normal component inhibits injection by moving the charge carriers to the detector bulk. As  $V_{bias}$  increases, the voltage drop between the rings also increases as a result of the normal component increase.



**Figure 4.** Ring potentials of neutron irradiated detector. Fluence was (a)  $5 \times 10^{13}$ ; (b)  $5 \times 10^{14}$ ; (c)  $3 \times 10^{15}$ ; (d)  $5 \times 10^{15}$   $n_{eq}/cm^2$ . The solid line shows the potential of the pad, the numbers of curves correspond to the numbers of the rings.

Indeed, figure 3 shows that  $V_{cr}$  increases with  $V_{bias}$ . In the limit, at sufficiently high  $V_{bias}$ , the path of hole transport between rings can be broken and injection will be terminated. Injection can be restored at larger  $V_{cr}$ . Therefore, an increase in  $V_{cr}$  with the bias voltage can be considered as a result of hole runaway from the injection path, which is equivalent to an increase in the potential barrier height.

According to the model, the criterion of the stable potential distribution in VTS is the injection current flow in VTS. In this case, the injection conditions will be individual for each ring spacing. The current flowing in certain ring spacing, being a bulk generation current will also be individual and will increase when approaching the pad due to summing of the currents of outer rings.

## 5. Influence of neutron irradiations on potential distributions in VTS

As was shown in the study of the mechanisms of the potential distribution in VTS before irradiation, the value of the electric field in the ring spacing is the most important factor, which determines the

potential distributions. Irradiation of silicon detectors brings about the generation of radiation defects with energy levels that affect the effective space charge density  $N_{eff}$  in the SCR and the corresponding profile of the electric field. In the case of irradiation of n-Si, compensation with acceptor levels mainly occurs; therefore, at low fluences  $\Phi$ , the  $N_{eff}$  in the SCR decreases. At higher  $\Phi$ , the sign of the space charge is changed from positive to negative, i.e., space charge sign inversion takes place. The dependence of the effective concentration  $N_{eff}$  on the neutron fluence  $\Phi$  can be calculated using the following parametric equation [9]:

$$N_{eff}(\Phi) = N_{d0} \cdot \exp(-\gamma \cdot \Phi) - \beta \cdot \Phi, \quad (1)$$

where  $N_{d0}$  is the effective space charge density before irradiation with  $N_{d0} = N_{eff}(\Phi = 0)$ ;  $\gamma = 8.8 \times 10^{-14} \text{ cm}^2$  is the donor removal rate; and  $\beta = 0.022 \text{ cm}^{-1}$  is the acceptor introduction rate. According to equation (1), inversion occurs at  $\Phi = 1 \times 10^{13} \text{ n}_{eq}/\text{cm}^2$  for the silicon with the resistivity  $7 \text{ k}\Omega\text{-cm}$  ( $N_{d0} = 6 \times 10^{11} \text{ cm}^{-3}$ ) used in the study. As the radiation fluence is further increased, the magnitude of  $N_{eff}$  increases.

The operation of the VTS radically changes at a fluence of  $5 \times 10^{13} \text{ n}_{eq}/\text{cm}^2$  (figure 4 (a)).  $V_{cr}$  becomes equal to zero for all rings, while the dependences of the ring potentials on  $V_{bias}$  are significantly linearized. The space charge is negative and the electric field maximum is located near the  $n^+$  contact; at a voltage lower than the full depletion voltage for the structure, the rings on the  $p^+$  side are found to be in the zero electric field. Indeed, in a partially depleted detector, the conducting base near the  $p^+$  contact connects all the rings to each other; the leakage current of the  $n^+$ - $n$  junction flows over the edge of the detector and then through the VTS, thus increasing the potential of the outermost ring and then of all rings. Therefore, in the case of full depletion of the detector (more than 75 V), a drop in the potential arises between the rings according to the standard punch-through mechanism, however, now at a level of nonzero potential of the outermost ring.

At a fluence of  $5 \times 10^{14} \text{ n}_{eq}/\text{cm}^2$ , an increase in the potentials of all rings is observed; as a result, the drop in the voltage at the periphery of the detector reaches a value of more than 50 % of the voltage  $V_{bias}$ . It is noteworthy that, in this case, the potentials of the rings increase virtually linearly in the entire range of voltages; an appreciable difference between the potentials of neighboring rings arises at  $V_{bias} > 200 \text{ V}$  (figure 4 (b)). This value is found to be several times smaller than the full depletion voltage, which, according to [10], is equal to about 750 V. This fact is a direct evidence of the existence of two maxima for the electric field in heavily irradiated  $p^+$ - $n$ - $n^+$  detectors; these maxima are located near the opposite contacts [11]. The main depleted region, on which a larger portion of the applied voltage drops, is situated near the  $n^+$  contact. An additional region of the electric field at the  $p^+$  contact is formed due to the capture of holes thermally generated in the bulk of the structure and is the cause of the appearance of a potential difference between the rings. It is evident that a difference in the ring potentials is insignificant since the potential drop at SCR of the  $p^+$  contact is several times smaller than that at SCR of the  $n^+$ -contact.

At higher fluences,  $3 \times 10^{15} - 5 \times 10^{15} \text{ n}_{eq}/\text{cm}^2$ , the trend in the potentials variation becomes reverse (figures 4 (c), 4 (d)). As a fluence increases, the potentials of the rings decrease and an effective division of the potentials is lacking. For example, at a fluence of  $5 \times 10^{15} \text{ n}_{eq}/\text{cm}^2$ , 80 % of the potential drops between the pad and the 1<sup>st</sup> ring. The reason for such a large difference between the potential of the pad and the 1<sup>st</sup> ring may be the dominance of the current related mechanism of the electric field formation in the bulk of the detector. The leakage current in the structure increases in proportion to the radiation fluence and, at  $\Phi \sim 10^{15} \text{ n}_{eq}/\text{cm}^2$ , reaches tens of  $\mu\text{A}/\text{cm}^2/300 \mu\text{m}$ . At a high generation rate in the bulk and a significant concentration of radiation defects, which are trapping centers for free charge carriers, the electric field profile is formed by the trapped charge of electrons and holes, i.e., this field mainly exists in the regions where the current flows. On the  $p^+$  side, these include the region adjacent to the sensitive  $p^+$ - $n$  junction where the main current of the detector is collected. Thus, the VTS rings surrounding this region and isolating it from the pad do not collect current and are situated away from the path of holes drifting toward the  $p^+$  contact. VTS is situated in the region with a low electric field and the potential is close to that of the ohmic  $n^+$  contact. This is completely consistent with the conditions of the performed experiment since, at the highest fluence ( $5 \times 10^{15} \text{ n}_{eq}/\text{cm}^2$ ), the thickness of

the SCR on the  $n^+$  side does not exceed  $100 \mu\text{m}$  at  $V_{bias} = 400 \text{ V}$ . Therefore, the electric field distribution is determined by the path of the current flow in the base; this current forms the space charge by the mechanism of charge carrier trapping. Qualitatively, the relation between the electric field distribution and the flowing current is given by the following expression:

$$divE \sim qN_{tr} \sim f(\tau)(j_p - j_n), \quad (2)$$

where  $q$  is the elementary charge;  $N_{tr}$  is the difference between the concentrations of captured electrons and holes;  $f(\tau)$  is a function describing the probability of the capture of electrons and holes; and  $j_p$  and  $j_n$  are the electron and hole current densities, respectively. Since the hole current is dominant at the  $p^+$  contact, the value of  $divE$  is always positive; consequently, the maximum electric field is bound to be located at the surface of the  $p^+$  contact, which collects holes. The electric field strength near the isolated rings is bound to be at a minimum and, as experiments show, their potential is close to that of the  $n^+$  contact (figure 4 (d)).

## 6. Conclusions

The developed physical model of the potential distribution in VTS considers both the current flow in the SCR and electrostatic aspects. The model can be applied to the development of floating ring structures on high purity materials.

The radiation induced degradation of a detector bulk led to a disruption in the operation of the VTS. The dominant mechanism in the case of the fluence increase is the variation in the electric field distribution in the detector bulk and the replacement of the electrostatic mechanism for field formation in the SCR by a mixed mechanism with a dominant influence of the density of the electron-hole generation current, which flows in the bulk. In this situation, the potential that dropped in the VTS is reduced and becomes substantially lower than the voltage applied to the structure, i.e., the VTS loses the properties of a system that optimizes the potential distribution.

In silicon radiation detectors, which operate at high radiation fluences and high voltages, the observed stability of their characteristics (i.e. without breakdown) is governed by the space charge limited current, i.e., by suppression of the electric field in regions where the subthreshold high electric field gives rise to the injection of charge carriers from the contact to the detector bulk. This conclusion confirms this mechanism, which was suggested previously by V. Eremin, et al. [12].

## Acknowledgments

This study was supported by the grants of the Scientific School of the President of the Russian Federation (grants no. NSh\_3306.2010.2, 3308.2012.2), by the program “Experimental and Theoretical Studies of Basic Interactions Related to Experiments at the Accelerator Complex CERN”, and is in the frames of the scientific program of CERN-RD50 collaboration.

## References

- [1] Koa Y C and Wolley E D 1967 Proc. IEEE **55** 1409-14
- [2] Adler M S, Temple V A K, Ferro A P and Rustay R C 1997 IEEE Trans. Electron Devices **ED-24** 107-13
- [3] Baliga B J 1990 Sol. St. Electron. **33** 485-8
- [4] Suh K D, Hong S W, Lee K and Kim C 1990 Sol. St. Electron. **33** 1125-9
- [5] Brieger K P, Gerlach W and Pelka J 1983 Sol. St. Electron. **26** 739-45
- [6] Bae D G and Chung S K 2000 Sol. St. Electron. **44** 2109-16
- [7] Boisson V, Helle M Le and Chante J P 1985 IEEE Trans. Electron Devices **ED-32** 838-40
- [8] Eremin V, Verbitskaya E, Ilyashenko I, Eremin I, Safonova N, Tuboltsev Yu, Egorov N, Golubkov S and Konkov K 2009 Semiconductors **43** 796-800
- [9] Li Z, Dezillie B, Chen W and Bruzzi M 2002 Nucl. Instrum. Meth. A **476** 628-38
- [10] Sze S M 1969 Physics of Semiconductor Devices (New York: Wiley-Interscience)
- [11] Eremin V, Verbitskaya E and Li Z 2002 Nucl. Instrum. Meth. A **476** 537-49
- [12] Eremin V, Verbitskaya E, Zabrodskii A, Li Z and Härkönen J 2011 Nucl. Instrum. Meth. A, **658** 145-51